



# Flooding, channel dynamics and transverse infrastructure: a challenge for Middle Ebro river management

Jesús Horacio, Alfredo Ollero, Iván Noguera & Víctor Fernández-Pasquier

To cite this article: Jesús Horacio, Alfredo Ollero, Iván Noguera & Víctor Fernández-Pasquier (2019) Flooding, channel dynamics and transverse infrastructure: a challenge for Middle Ebro river management, Journal of Maps, 15:2, 310-319, DOI: [10.1080/17445647.2019.1592719](https://doi.org/10.1080/17445647.2019.1592719)

To link to this article: <https://doi.org/10.1080/17445647.2019.1592719>



© 2019 The Author(s). Published by Informa UK Limited, trading as Taylor & Francis Group



[View supplementary material](#)



Published online: 01 Apr 2019.



[Submit your article to this journal](#)



Article views: 546



[View related articles](#)



[View Crossmark data](#)



Citing articles: 1 [View citing articles](#)



## Flooding, channel dynamics and transverse infrastructure: a challenge for Middle Ebro river management

Jesús Horacio<sup>a,b</sup>, Alfredo Ollero<sup>c</sup>, Iván Noguera<sup>d</sup> and Víctor Fernández-Pasquier<sup>e</sup>

<sup>a</sup>Department of Geography, Faculty of Geography and History, University of Santiago de Compostela, Santiago de Compostela, Spain;

<sup>b</sup>Laboratory of Environmental Technology, Institute of Technological Research, University of Santiago de Compostela, Santiago de Compostela, Spain; <sup>c</sup>Department of Geography and Regional Planning, University of Zaragoza, Zaragoza, Spain; <sup>d</sup>Department of Geo-environmental Processes and Global Change, Pyrenean Institute of Ecology, CSIC, Zaragoza, Spain; <sup>e</sup>Technical Advisor in Aquaculture

### ABSTRACT

This study documents the impacts of engineering works on flood risk and channel dynamics of the maximum geomorphic flow reach of the Middle Ebro River (Spain) over the last ninety years. The map reveals how the construction of transversal transport lines and their ineffective design and maintenance has contributed to an elevated risk of flooding and channel avulsion at this location. In addition, the development of flood protection structures has restricted the natural dynamics of the river. These modifications have restricted the passage of flood waters, ultimately increasing flood hazards, by changing the area and depth of inundation and extending the flood hydrograph. The map allows for the interpretation of key processes, forecasting of flood hazards, and the evaluation of possible mitigating actions. These findings reconfirm that reducing space for the mobility of a river is not a good management solution and further aggravates the current situation.

### ARTICLE HISTORY

Received 8 September 2018

Revised 28 February 2019

Accepted 6 March 2019

### KEYWORDS

Floods; risk; anthropization; room for river; land planning; environmental management

## 1. Introduction

Rivers adjust and self-organize their geomorphologic function as a response to natural processes and anthropic disturbances (Piégay, 2016). The middle reach of the Ebro River (NE of the Iberian Peninsula, Spain; Figure 1) is a free meandering course of ~350 km characterized by an extensive floodplain (maximum width of the study area is 4.7 km) with agricultural and residential land-use, a low riverbed slope ( $0.00065 \text{ m}\cdot\text{m}^{-1}$ ) and a dynamic channel. The dynamics of the reach are propelled by the confluence of the Aragon River, just upstream of the study site (Ollero, 1992). The Aragon River ( $105 \text{ m}^3\cdot\text{s}^{-1}$ ) almost doubles the flow of the Ebro River ( $224 \text{ m}^3\cdot\text{s}^{-1}$  downstream of the confluence), contributing to an increased flood hazard at the reach. The reach studied is representative of the most important geomorphic changes that have been recorded in the last century in the middle Ebro River (Ollero, 1991), hence the reason why it was declared as a protected site of the Natural Reserve of Sotos de Alfaro in 2001. A few kilometers downstream from the Aragon confluence, several types of transport infrastructure (railway lines, highways and motorways) traverse the channel and floodplain causing an impedance of flow during flooding, elevating flood risk. Consequently, the reach is considered ‘high risk’ in the Flood Risk Management Plan (PGRI) of the Ebro Hydrographic Confederation

(CHE, 2015), and has experienced the highest recorded flood,  $4,950 \text{ m}^3\cdot\text{s}^{-1}$  in December 1960, of anywhere in the catchment. This value is a record in the Ebro basin and one of the highest flow values measured on the Iberian Peninsula (Ollero, 1992).

Prior to river engineering works in the 20th century, the channels of the site naturally migrated over the floodplain with meander cut-offs and common avulsions (Pellicer & Ollero, 1987). These active dynamics began being restricted in the 1960s with the regulation of water flow and construction of engineering works (namely stopbanks<sup>1</sup>) to defend against flooding, and bank erosion (Díaz-Redondo, Marchamalo, Egger, & Magdaleno, 2018; Ollero, 1991). Despite the defences, floods commonly overtop the protection structures, damaging agriculture, closing the N-113 road and sometimes causing water intake problems in the locality of Alfaro. The infrastructure has also altered how floods pass through this reach, rendering the reach’s current gauging station ineffective at capturing a representative discharge. In the most recent floods, for example in February 2015, inundation, unexpected for the magnitude of these floods, is thought to have also resulted partly from intentional blockage of AP-15 highway culverts to divert flood waters, creating a social conflict between affected parties. As a result of all of these interventions, flood risk remains high, the boundary conditions are changing, and floods are difficult to forecast.

**CONTACT** Jesús Horacio ✉ [horacio.garcia@usc.es](mailto:horacio.garcia@usc.es) Department of Geography, Faculty of Geography and History, University of Santiago de Compostela, Praza da Universidade, 1, 15782. Santiago de Compostela, Galicia, Spain; Laboratory of Environmental Technology, Institute of Technological Research, University of Santiago de Compostela, Bloque A, Campus Universitario Sur, 15782. Santiago de Compostela, Galicia, Spain

© 2019 The Author(s). Published by Informa UK Limited, trading as Taylor & Francis Group

This is an Open Access article distributed under the terms of the Creative Commons Attribution-NonCommercial License (<http://creativecommons.org/licenses/by-nc/4.0/>), which permits unrestricted non-commercial use, distribution, and reproduction in any medium, provided the original work is properly cited.

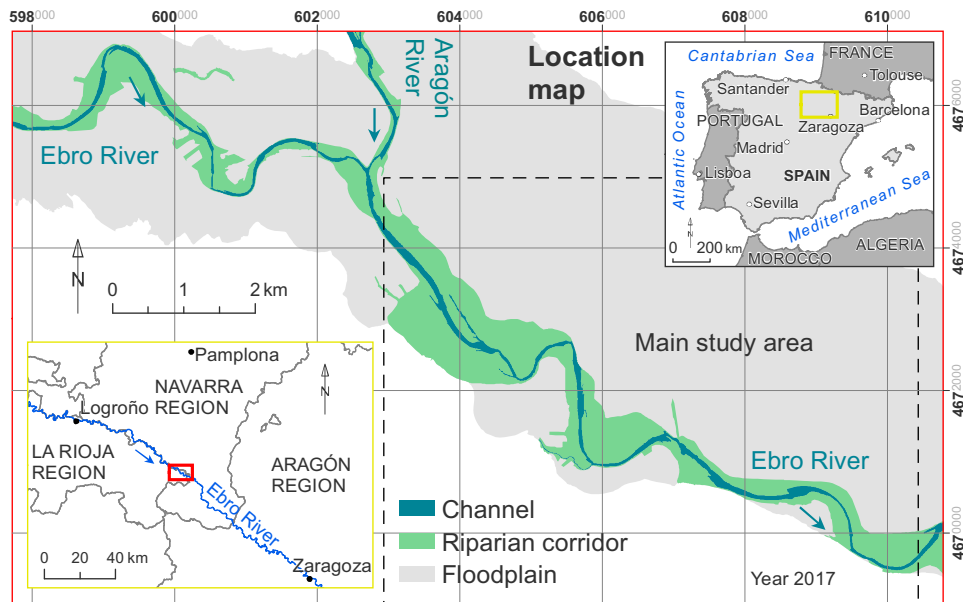


**Figure 1.** Location of the study area.

The purpose of the map produced here is to show the natural and current dynamics of the reach, the impacts of transverse infrastructure and the complex problems of land management, and to help convey the current flood hazards and possible solutions for flood mitigation (Hong & Chun, 2018). In Spain there are very few antecedents of this type of floodplain cartography that integrate natural and anthropic elements and processes (Ibáñez, Acín, Díaz, Granado, & Ollero, 2012). The presented case is unique, especially because of its dimensions, on a peninsular scale, but at the same time it shows a generalized problem in many rivers, the problem of unsuitable infrastructures for fluvial functioning. The map's resolution and legend can be extrapolated to other works and is a useful template for the planning of the territory and for watershed management and risks.

## 2. Method

### 2.1. Data collection

Existing datasets were collected, along with new datasets, to provide information on the anthropic elements

(AE), hydrological dynamics (HD), and the geomorphological dynamics (GD) of the channel and floodplain (Table 1).

Anthropic elements (AE) make reference to the most relevant human infrastructures such as villages; transport lines; agricultural, farming or industrial infrastructure; and structures oriented toward mitigating the risk of flooding. The mapping of these elements was carried out using the information contained in the Cartocity (urban cartography) layer, vector files of the latest updates of the National Topographic Map (transport lines and other infrastructures), and manual editing of other elements related to risk mitigation not collected in the official cartography (e.g. stopbanks, relief channels, plugged drainage piping). The existence and positioning of these infrastructures was validated with the 2017 orthophoto, LiDAR data and derived models, and through observations during fieldwork.

The hydrological dynamics (HD) represent the flood extension obtained from the hydrological-hydraulic models for the National System for Mapping Flood Areas in compliance with the EU Floods Directive (Directive 2007/60/EC). The T10, T50 and

**Table 1.** Data used for the development of the map and main characteristics: CHE = Ebro Hydrographic Confederation; CECAF = Cartographic and Photographic Center; IGN = National Geographic Institute; IDENA = Spatial Data of Infrastructure of Navarra; MAPAMA = Ministry of Agriculture, Fisheries and Food. Ministry for the Ecological Transition; GD = geomorphological dynamic; HD = hydrological dynamic; and AE = anthropic elements.

Data	Source	Date	Scale	Format	Goal
Aerial photo	CHE, CECAF, IGN, IDENA, IGN	1927, 1945, 1956, 1967, 1984-85	10K, 46K, 32K, ~19K, 30K	Image	GD
Orthophoto	IGN	2005, 2014, 2017	30K	Image	GD
National Topographic Map	IGN		25K	Vector	AE
LiDAR	IGN	2010-17	15K	LAS	GD, HD, AE
National System Mapping Flood Areas	MAPAMA	2011	25K	GRID	HD
Cartocity	IGN		25K	Vector	AE
Other anthropic elements	This study	2017	1K	Vector	GD, AE
Processes and trends	This study	1927-17	~1.5K	Vector	GD, HD

T500 return periods have been used to draw the inundation extents. These types of return periods represent floods with medium-high, very high and extreme risk, respectively.

The geomorphological dynamics (GD) were represented by mapping the river channel at eight time-steps according to the availability of aerial photography (1927, 1945, 1956, 1967, 1984, 2005, 2014, and 2017). The images used have different scales, color and resolutions. The images from the years of 1956, 2005, 2014 and 2017 were geo-referenced by the Administration (agencies responsible for management). The rest of the images were manually geo-referenced to the 2014 image (Table 1).

## 2.2. Cartographic development

The cartographic development was done entirely with ArcGIS 10.5 © ESRI software, and combines information that was (i) edited (GD and AE), (ii) re-edited (HD) and (iii) unedited (AE). The first refers to that directly drawn by the authors. The second to that which uses official information but was partially redesigned to fit the needs of the study. The unedited information maintains its original structure.

The process of re-editing the HD from the Mapping Flood Areas layer was aimed to continuously represent the flood area of the return period T10 (polygon) and the limit of the return periods T50 and T500 (polyline). The process was divided in three steps: (i) conversion of raster format to vector format; (ii) filling of all the gaps present within the floodable area (only for T10); and (iii) simplification of the perimeter using the Bend simplify algorithm (Wang, 1996) with a tolerance of 50 m (i.e. diameter of a circle that approximates a significant bend). Some areas of the Mapping Flood Areas layer (SNCZI, 2011) had to be manually

re-edited to fit the current conditions. The development of this layer is prior to, for example, the project for the high-speed rail. Any topographic modifications that occurred in the study area between 2010 and 2017 are not accounted for, with the present topography represented by the last national LiDAR flight (2017).

The GD were represented through two categories: (i) channel (referred to as riverbed); and (ii) riparian corridor (vegetation growing near a river), which is closely related to the active channel (Charlton, 2008). Four possible subcategories have also been mapped in these categories (Figure 2), two present in the channel: (a) bar (accumulation of non-vegetated sediments) and (b) island (islands or bars with aged vegetation or shrub); and two in the riparian corridor: (c) water body (e.g. an abandoned meander) and (d) anthropization (plantings in their different evolutionary manifestations). Within the same polygon the bar and island categories can co-exist, in the same way that a water body can exist within the anthropization category. The latter may also be present within a bar or island as long as there is no connection to the channel layer. The channel category and its subcategories were mapped at 1:1,000 scale. Those that reference the riparian corridor were made at 1:2,000 scale. In both cases we have supported our information of the aerial images with data derived from LiDAR, especially a slope model which was very useful in discerning the limits of each unit.

Due to the difference between the channel scale (1:1,000) and the riparian corridor (1:2,000) and the scale of representation of the main map (1:26,000) and auxiliaries (1:130,000), the subcategories (bar, island and water body, anthropization) do not appear in the main map. For the main map, both subcategory groups were merged with their corresponding parent-categories, but the sub-category information was

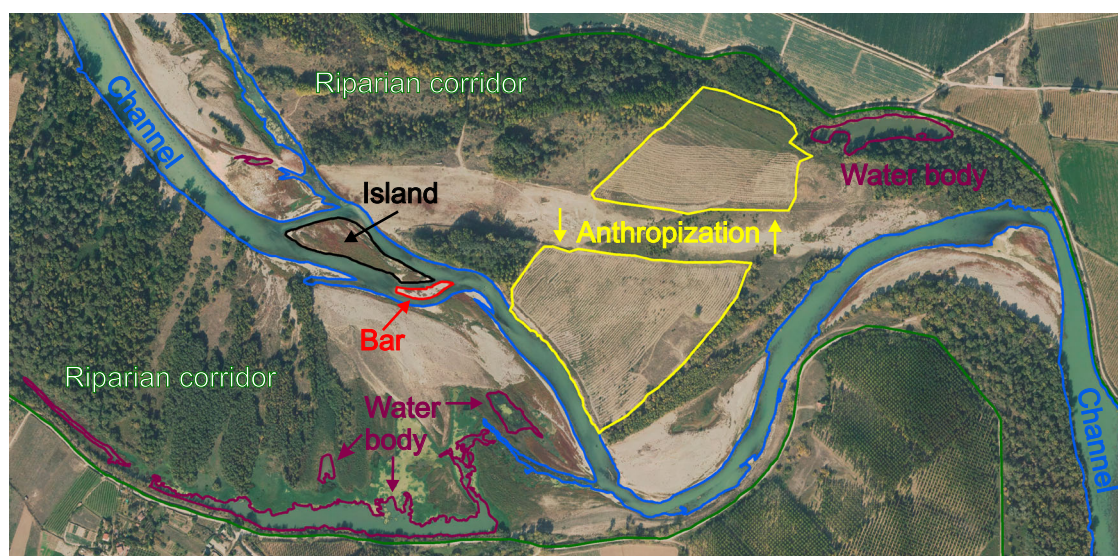


**Figure 2.** Representation in categories (channel and riparian corridor) and subcategories (bar and island, and water body and anthropization) of the geomorphological dynamics (GD).



taken into account in the calculation of the channel's evolution and riparian corridor changes (see section named *Discussion and conclusions*). To further improve efficiency in the reading and usefulness of the map, the polygons of the GD have been generalized following minimum mapping unit criteria (MacEachren, 2004):

$$MMU = (Lpv * E * 3)^2 = (0.0002 * 30,000 * 3)^2 \\ = 324 \text{ m}^2$$

where, MMU is the minimum mapping unit ( $\text{m}^2$ ), Lpv is the limit of visual perception (0.2 mm in the map, therefore, 0.0002 m) and E is the adjustment scale. Replacing the values, we obtained a MMU of  $324 \text{ m}^2$ . This means that all polygons smaller than  $324 \text{ m}^2$  were merged with the neighboring polygon with the longest shared border.

The quality of the final map was influenced by differences in the properties of the individual images used to generate the map. The problems introduced by these image differences were grouped into four types:

- Various flights for one image timestamp. For example, the imagery named 1984 was not collected all in the same year, and for the 1927 imagery, the photos were captured in two separate flights in that year. This means that for these images, (i) there are changes in the flow levels (water layer), islands and bars; and (ii) poor overlap of images during the geo-referencing.
- Low quality of the (1945, 1984, 1967) images and changes in luminosity (of the 1967 image). These maps make recognition and mapping of types and categories inconsistent between images.
- High arboreal vegetation on the edge of the channel, causing a 'visor effect' that has prevented the mapping of the boundary between the channel and the riparian corridor. This affects all images.
- Problems in obtaining stable checkpoints for geo-referencing, mostly affecting the 1927, 1945, 1967, and 1984 images. This was especially critical for the 1927 image. As a solution, the following steps were taken: (i) plot the cartography of each photoplane individually, omitting its geo-reference (each mapped sector was coded with the photoplane number); (ii) take a clearly identifiable stable checkpoint in time as a reference between the 1927 and 2014 images. This point corresponds to the photoplane of the easternmost study area (XY: 608,806.110; 4,670,079.115 m); (iii) based on the position of the cartography of the first photoplane, the rest of the photoplanes were added following the longitudinal continuity of the river; (iv) editing of the contact between those photoplanes that required an adjustment for the longitudinal

continuity of the channel and the riparian corridor. This mainly occurred, in the cartographic union of the two photoplanes pertaining to different flights. The peculiarities in the georeferencing of the 1927 flight have reduced the precision of adjustment between map and reality. Nonetheless, for the GD the most important value is not the exact position (within certain thresholds), but the representation of the spatial displacement of the channel and the change in the riparian corridor area. In this sense, we can say that the result adjusts to the problem proposed in the study.

### 3. Discussion and conclusions

#### 3.1. Overview

The coexistence of society with the rivers has led to deterioration of the natural state of rivers (Dynesius & Nilsson, 1994; Tockner & Stanford, 2002), but also to an increase in risk and spending of public investment to alleviate damages (Kind, 2014; Ocio, Stocker, Eraso, Martínez, & Sanz de Galdeano, 2016; Vinet, 2010). The geomorphological dynamics of a river is something inherent to the nature and quality of a river (Kondolf, Piégay, Schmitt, & Montgomery, 2016), however the dynamism of many rivers has been reduced in recent decades due to human interests. Infrastructure, occupation of floodplains, and defences have constrained many rivers, reducing the space available for them to move (Díaz-Redondo et al., 2018; Fuller & Basher, 2013; Ollero, 2010).

The restricted space of the Ebro River and the attempt at *domestication* through defence infrastructures is supported by a management model that prioritizes the occupation of the alluvial plain with agricultural, residential, or transport uses. Added to this loss of dynamics and complexity of the river are (i) the problem of the risk, which has been aggravated by increasing exposure and vulnerability even in a situation where the flood hazard remains constant; and (ii) the occupation of the alluvial plain with transport lines that traverse the river and its floodplain, which can impede flow and elevate the flood hazard. The map presented in this study shows that humans have elevated the risk of flooding at this reach of the Ebro River by both (i) and (ii) above. Appropriate design of transport lines that cross the waterways is a necessary part of flood management (Alcarria, Castillo, & Pagés, 2006; Blanton & Marcus, 2009; Johnson, 2002), with the need to make these transversal elements sufficiently permeable to allow the passage of water and to prevent significant ponding or flow resistance; however, this does not seem to have been achieved at this reach, with the linear infrastructure significantly changing the flood hazard. Both in the RD 903/2010 and in the Flood Risk Management Plan, approved for all of

Europe in 2015, measures to improve the drainage of linear infrastructures, especially roads and railways, were recommended. These measures are usually the opening of spillways under the infrastructures and the widening of the active channel under the bridge, pushing back the stopbanks. In the Ebro River Flood Risk Management Plan (CHE, 2015), however, only one action is proposed in another bridge located 70 km downstream of the study area.

The map also shows how the encroachment of infrastructure and control measures at this site has modified the river's dynamics, shown by the invasion of fluvial space in the riparian corridor and in the channel with the regulation and control infrastructures (Figure 3). The changes that the Ebro River has experienced in recent decades are the result of its continual adjustment to fluctuations in water and sediment transport. Lateral mobility of the channel was up to ~1.5 km in one sector of the reach during the study period. However, the migration of the channel and the mobility of bars and islands that occurs with each flood, have been restricted more and more by the stopbanks and artificial-fixtures that impinge upon the channel, thus constraining the natural dynamics of the river in its processes and forms. The riparian corridor area was reduced by 45.4% over the period from 1927 to 2017. Using the year 1927 as a reference, we observe how in the year 1984 almost 60% was lost, while the loss in 2005 and 2014 is ~50%. The only increase in the riparian corridor occurred between 1927 and 1945, with an increased surface area of 6.6%. The reason for this increase is the effect of the floods of the 30's. They were not extraordinary but they were frequent, capable of generating erosion and slight changes (especially on the right margin) that forced farmers to retreat. During the Civil War (1936–39) and later years, the agricultural invasion of the riverbed slowed down. The channel is characterized by a marked simplification of its active channel and sinuosity. Between 1927 and 2017 the surface of the channel dwindled more than 55%, while also gaining a significant increase in the straightening of a sector

which would be meandering in otherwise natural conditions.

### 3.2. Applicability of the map

In the past, the maps were exclusively descriptive, to reveal changes in the river landscape (Apan, Raine, & Paterson, 2002). Subsequently, risk maps have been developed, which are fundamentally flood-prone and do not usually assess the exposed elements (Bücheler et al., 2006), although there are very interesting contributions in Spain by Bescós and Camarasa (2004) and Camarasa and Soriano (2012). In recent years, the greatest effort has focused on cartographic techniques supported by LiDAR or VHR imagery or UAV (Demarchi, Bizzi, & Piégay, 2016; Dietrich, 2016; Jones, Brewer, Johnstone, & Macklin, 2007; Langhammer & Vacková, 2018; Rusnák, Sládek, Kidová, & Lehotský, 2018; Wheaton et al., 2015). Only in very recent cases are legends intended to lay stable foundations (Miklín & Galia, 2017; Montané, 2014).

The product achieved goes a step further in the integration of elements, processes and management alternatives. Our map is a useful tool for management since it clearly shows the problems and allows for a discernment of solutions. This product is, therefore, richer than conventional risk mapping. For example, the detailed map of Figure 4 allows the identification of black spots in floods and can be used by the hydrological administration and civil protection for monitoring upcoming processes with overflowing flows.

### 3.3. Processes and flood tendencies

The interpretation of the processes, the forecast of trends and the evaluation of potential mitigation actions in the study area are closely related to the effect of the transversal transport lines, mainly the AP-15 highway and its flood management. The route and the bridge of the AP-15 highway over the Ebro River already generated problems from the moment of its construction in 1978. The rapid migration of the meander of the Ebro River developed immediately upstream of the bridge in the floods of 1977, 1978, 1980 and 1981 (Ollero, 2010), jeopardizing the base of the left bank of the river and the embankment of the highway. This called for the construction of an expensive canalization of the Ebro River, with a public investment of ~12 million euros to realign the channel and avoid demolition of the bridge. The work was carried out in 1986 and 1987 (Ollero, 1992). At present, the problem focuses on the blockage in 2013 of the drainage culverts under the AP-15 highway by the farmers downstream from the infrastructure. This makes the embankment of the highway behave like a transversal dike to the Ebro River and increases the upstream flood hazard. At present, the spillways remain

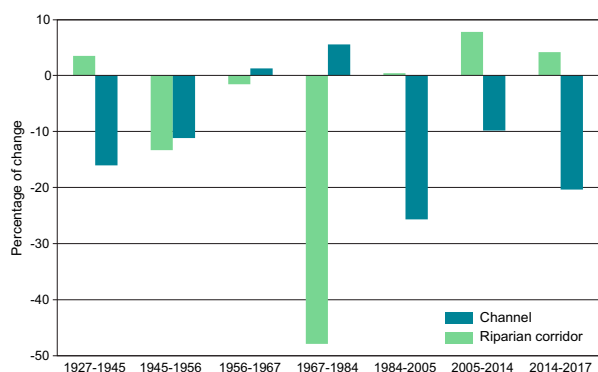


**Figure 3.** Changes in area of active channel 1927–2017 (channel and riparian corridor).

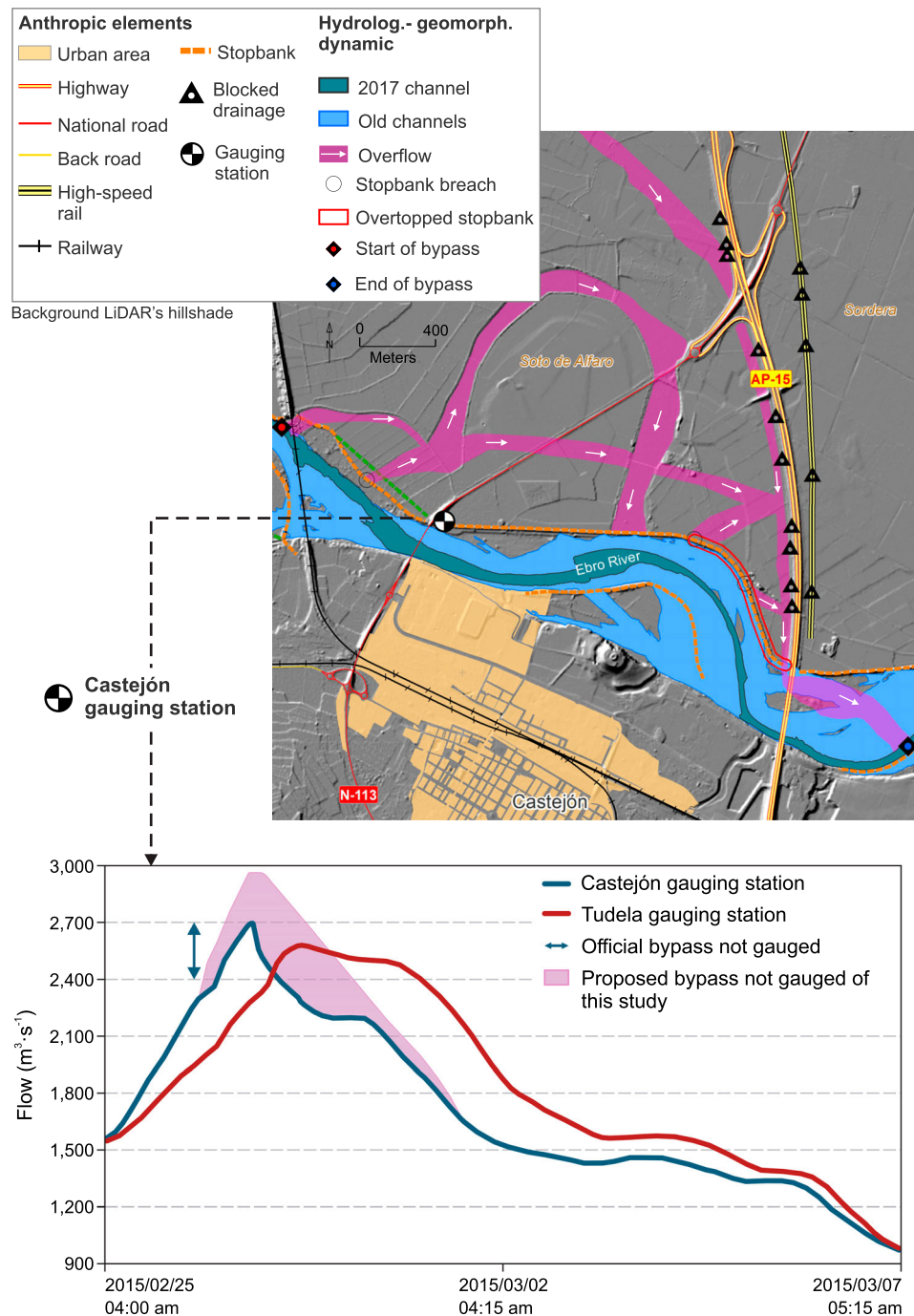


**Figure 4.** Flows measured during the flood of February-March 2015. In the graph it is observed how the gauging station of Tudela (located ~22 km downstream; ~15 km in a straight line) recorded more flow than the gauging station of Castejón ( $157.5 \text{ m}^3 \cdot \text{s}^{-1}$ ). The curve of Tudela is close to the curve of Castejón from 07:00 am on February 27th until 05:00 am on March 7th. The extra flow corresponded for the most part to the failure in the capacity of Castejón, i.e. to the important water bypass of overflowing water that was not quantified in the gauging station, but which circulated through the floodplain to return to the main channel of the Ebro River at the height of the AP-15 highway bridge.

inoperative and the requests of the owners upstream to reinstate the culverts have not been met.

The floods in 2015 showed the effects caused by the waterproofing (i.e. blocking of the culverts) of the AP-15 highway, similar to the effects of the elevated railway upstream. In February of that year the Ebro River had three major floods, two consecutive and a third 22 days later. The peak flows generated downstream from the Ebro-Aragon junction breached the stopbank in several places in front of Castejón, specifically between

the railway bridge and the highway. These two consecutive transversal infrastructures funnel the flooded waters into the active channel, increasing the flow there. The water that circulates on the floodplain pools against the highway embankment. A component of the flow is directed northward, flooding the fields of Cadreita. This generates a large pool that grows in surface and depth to be considerably greater than that which exists in a natural flood (prior to the instalment of the transverse infrastructure). A second branch of

the flow presses towards the lower riverbed of the Ebro River, towards the highway bridge, looking for a topographic exit.

These break-out channels on the floodplain take advantage of traces of former channels of the Ebro River that are currently cultivated but slightly lower topographically. These waters bypass the main channel and therefore do not pass through the gauging station of Castejón. This means that the flow data recorded by this station is not representing all of the flow during these floods, biasing the flood hydrograph at this location. During a flood in 2015 the Automatic Hydrological Information System (SAIH) recorded a peak flow of  $2,400 \text{ m}^3 \cdot \text{s}^{-1}$ , but the Ebro Hydrographic Confederation (CHE) has subsequently increased it to  $2,690 \text{ m}^3 \cdot \text{s}^{-1}$ , evaluating the non-graduated bypass at  $290 \text{ m}^3 \cdot \text{s}^{-1}$ . Based on our mapping of the flood inundation, we have estimated that the flow that bypassed was in fact more likely to be  $\sim 500 \text{ m}^3 \cdot \text{s}^{-1}$ , giving a total peak flood magnitude of Castejón  $\sim 2,900 \text{ m}^3 \cdot \text{s}^{-1}$  (Figure 4).

Where the diverted flow rejoins the main channel, the additional flow elevates the main channel and causes the stopbank to breach. Once the flood level begins to lower, a gradient is formed in the active channel that takes advantage of most of the mass of water that is stored, as well as the one that circulated through the floodplain, to return under the bridge of the AP-15 to the main Ebro River. In its return the flow overtops about 95 meters of the flood protection structure, just upstream from the bridge. At this point a constant flow of  $\sim 500 \text{ m}^3 \cdot \text{s}^{-1}$  is generated during  $\sim 35 \text{ h}$ , corresponding to the emptying time of the temporary floodplain storage. This additional flow explains the difference in shape between the hydrographs from the gauging station of Tudela, located  $\sim 22 \text{ km}$  downstream ( $\sim 15 \text{ km}$  in a straight line), and that of the gauging station upstream at Castejón. The persistence of unusually high flow during the  $35 \text{ h}$  (second peak) explains the plateau in the Tudela hydrograph (Figure 4).

The second peak of the flood surprised the riverside towns, resulting in contradictory information and actions by the Administration and, consequently, altering the evacuation tasks. In the flood recorded in the spring of 2018 a very similar situation occurred again, so CHE considers giving more validity to the gauging station of Tudela for its greater reliability.

### 3.4. Conclusions: evaluation of proposals and perspectives from mapping to river management

The cartography which has been created tries to identify and represent all the relevant natural and human aspects in a high-risk situation of intense fluvial dynamics. This applied cartography is useful (i) to

explain the problem, (ii) to help the managers of the territory determine possible risks in the decision-making in upcoming extreme events (Hong & Chun, 2018), and (iii) also to recommend proposals in search of solutions. The map also incorporates the defense and management actions that are being carried out in the area, which is why it is an active cartography, presented as a constantly updated product. The product is exportable to any other reach of the floodplain with significant flood risk. But the legend is open to the incorporation of new elements or actions that intervene in fluvial processes and risk. At the applied scientific level, the map also represents a step forward in fluvial geomorphology, floodplains, flooding and rehabilitation. As an example of all this, the proposals and perspectives raised in the case study are presented below.

The blocked drains of the AP-15 highway (Figure 5A), added to the dam effect they exert and to the effect that the railway has upstream, have caused a dangerous increase of the risk situation due to: (i) the alteration of the normal flooding processes, (ii) the prolongation of its times and the flooding downstream, (iii) the distortion of the flow data and (iv) the consequential problems in decision-making. This situation will be equally serious in future floods especially if these are extraordinary, as has been observed in the events of April 2018.

Despite the effects generated by the flood at the end of February 2015, the Flood Risk Management Plan of the Ebro Basin, which was approved and published in January 2016, did not mention the problem and only collected among its actions the permeation of the Pradilla-Boquiñeni bridge, located  $70 \text{ km}$  downstream, with a budget of 1.3 million euros. The only actions carried out in the area to date have been to rebuild the stopbanks and raise them between 40 and 60 cm in the sectors where important flow entries and exits were observed. An embankment has also been placed on the AP-15 highway at a point where the reservoir and overflow water pressure were about to destroy it. A drain siphon existed at this point which was clogged up (Figure 5A). These actions can worsen the situation in the next floods and do not solve the problem, but only serve to further enclose the flood flows.

The measures that should be undertaken in the short term have to be focused along two lines. First, it is imperative to improve permeability of the entire AP-15 embankment on the floodplain of the Ebro River, reopening the drainage culverts currently clogged and adding additional new capacity by installing more and larger culverts. Increased capacity will reduce flow concentrations and subsequent fluvial scours, limit flooding upstream and facilitate a faster receding flood limb. Ideally, the entire highway, or any new infrastructure should cross the floodplain on pillars instead of over an embankment. Second, moving





**Figure 5.** Dam effect of the AP-15 highway and drainage siphon plugged up with the works of 2015 (© CHE, 2015. Aerial flight tracking the Ebro flood in February 2015); the image can be located in the main map in the overflow of the Soto de Alfaro meander (see also Figure 4) (5A). Works in the relief channel in 2015; the image can be located in the main map (downstream section of the relief channel) (5B). Erosion of a stopbank in 2018, which was made to protect the riverbank a few months before (© Diario La Rioja); the image can be located in the main map seeing the Estajao stopbank (5C).

the stopbanks outwards would give greater space to the passage of flood waters, especially considering that in this section of the river Ebro the highest peak flows are reached. Both actions would help to reduce risk and contribute to better functioning of the river in floods.

In autumn of 2015 the CHE also began working on a relief channel (Figure 5B) to improve the water circulation in flooding and reduce the pressure on the water intake in the village of Alfaro. This channel was already operative in 2016 and constitutes the first use of this type of mitigation in the Middle Ebro River, but with an experimental character. At the same time, CHE has also been working, with the support of several groups, in the application of a LIFE project, 'Ebro Resilience' (LIFE17 TAE/ES/000003). The project proposes the repositioning of three stopbanks: Chorro de la Nava, Estajao and La Roza. Besides, the relief channel has shown an irregular operation in the recent flood of April 2018, driving the flow against the left bank and generating some breaks in the structure. Therefore,

it seems that the management policy for the next years is going to prioritize the repressing of these structures to give more space to the river. The relief channel is going to be given a secondary role or can even be abandoned, especially because they are, on the one hand, working on the opening of new water intake for Alfaro, far from the channel, and on the other hand, on the closing of the current one.

After the flood of April 2018, and over a period of 2 months, the Ebro River has maintained a high flow without overflow that has generated significant erosion on the bank where the current water intake (Figure 5C) is located. This erosion has removed more than 25 m of the width of sediment that was deposited in 2016 in this margin reusing the sediments extracted from the relief channel. Knowing that this riverside will be unprotected in the future with the setback of the Estajao stopbank, Alfaro's city council is demanding a 'hard' protection until the water intake is closed down and another opens. Nonetheless, this type of work continues to prove itself useless and poses a

waste of public money, when simply, it would be much easier to work ‘with the river’ rather than ‘against the river’.

## Software

ESRI ArcGIS 10.5 and QGIS 2.18.19 were used for map data visualization, metric analysis and layout creation. The Mapping Flood Areas layer was made using HEC-RAS software (U.S. Army Corps of Engineers).

## Note

1. Other terms in the scientific literature to define stop-bank (flood protection structure): levee dike, dyke, embankment, floodbank.

## Acknowledgments

The authors wish to show their sincerest gratitude to José Ángel Losada (Hydrographic Confederation of the Ebro) and the entire team at the National Geographic Institute for public relations for their kindness and efficiency in the request of information and clarification of doubts; to the local agents Alberto Lasheras (Cadreira), María Jesús Ramón and José María Hernández Romero (Alfaro), as well as other members of the Hydrographic Confederation of the Ebro, for the relevant information offered; to Victor Bouzas Blanco for his comments on the map; to Alissa Jensen for her contribution in English; to Ian Fuller and Sam McColl for their valuable comments to improve the article; to Belize Lane, Juliane Cron, and Luca Franzi as reviewers of the manuscript, and Tobias Heckmann, as Associate Editor, for their comments and suggestions.

## Disclosure statement

No potential conflict of interest was reported by the authors.

## Funding

The first author is the beneficiary of the postdoctoral fellowship *Programa de ayudas de apoyo a la etapa inicial de formación posdoctoral* (2017) awarded by the Consellería de Cultura, Educación e Ordenación Universitaria de la Xunta de Galicia (Government of Galicia, Spain).

The third author is the beneficiary of the pre-doctoral fellowship *Ayudas para la contratación de personal investigador predoctoral en formación* (2017) awarded by the Gobierno de Aragón (Government of Aragón, Spain).

This study is integrated within projects CGL2014-52135-C3-3-R and CGL2017-83866-C3-1-R, financed by the Ministerio de Economía y Competitividad (Ministry of Economy and Competitiveness, Spain); Universidad de Zaragoza.

## References

- Alcarria, J., Castillo, O., & Pagés, J. (2006). Recomanacions tècniques per al disseny d'infraestructures que interfereixen amb l'espai fluvial. Agència Catalana de l'Aigua, Barcelona.
- Apan, A. A., Raine, S. R., & Paterson, M. S. (2002). Mapping and analysis of changes in the riparian landscape structure of the Lockyer Valley catchment, Queensland, Australia. *Landscape and Urban Planning*, 59, 43–57.
- Bescós, A., & Camarasa, A. M. (2004). La creciente ocupación antrópica del espacio inundable y el aumento de la vulnerabilidad en las poblaciones del Bajo Arga (Navarra). *Boletín de la Asociación de Geógrafos Españoles*, 37, 101–117.
- Blanton, P., & Marcus, W. A. (2009). Railroads, roads and lateral disconnection in the river landscapes of the continental United States. *Geomorphology*, 112, 212–227.
- Büchle, B., Kreibich, H., Kron, A., Thielen, A., Ihringer, J., Oberle, P., ... Nestmann, F. (2006). Flood-risk mapping: Contributions towards an enhanced assessment of extreme events and associated risks. *Natural Hazards and Earth System Sciences*, 6, 485–503.
- Camarasa, A. M., & Soriano, J. (2012). Flood risk assessment and mapping in peri-urban Mediterranean environments using hydrogeomorphology. Application to ephemeral streams in the Valencia region (eastern Spain). *Landscape and Urban Planning*, 104, 189–200.
- Charlton, R. (2008). *Fundamentals of fluvial geomorphology*. London and New York: Routledge. 234 pp.
- CHE - Confederación Hidrográfica del Ebro. (2015). Plan de gestión del riesgo de inundación. Demarcación Hidrográfica del Ebro.
- Demarchi, L., Bizzi, S., & Piégay, H. (2016). Hierarchical object-based mapping of riverscape units and in-stream mesohabitats using LiDAR and VHR imagery. *Remote Sensing*, 8, 97. doi:10.3390/rs8020097
- Dietrich, J. T. (2016). Riverscape mapping with helicopter-based structure-from-Motion photogrammetry. *Geomorphology*, 252, 144–157.
- Díaz-Redondo, M., Marchamalo, M., Egger, G., & Magdaleno, F. (2018). Toward floodplain rejuvenation in the middle Ebro River (Spain): From history to action. *Geomorphology*, 317, 117–127.
- Dynesius, M., & Nilsson, C. (1994). Fragmentation and flow regulation of river systems in the northern third of the world. *Science*, 266, 753–762.
- Fuller, I. C., & Basher, L. R. (2013). Riverbed digital elevation models as a tool for holistic river management: Motueka River, Nelson, New Zealand. *River Research and Applications*, 29, 619–633.
- Hong, C., & Chun, H. (2018). Barriers, challenges, conflicts, and facilitators in environmental decision-making: A case of An'Yang Stream restoration. *River Research and Applications*, 34, 472–480.
- Ibáñez, A., Acín, V., Díaz, E., Granado, D., & Ollero, A. (2012). Cartografía geomorfológica: herramienta de análisis de la dinámica fluvial en ríos aluviales. In A. González Díez (coord.), *Avances de la Geomorfología en España. Actas de la XII Reunión Nacional de Geomorfología* (pp. 505–508). Santander: Universidad de Cantabria.
- Johnson, P. A. (2002). Incorporating road crossings into stream and river restoration projects. *Ecological Restoration*, 20(4), 270–277.
- Jones, A. F., Brewer, P. A., Johnstone, E., & Macklin, M. G. (2007). High-resolution interpretative geomorphological

- mapping of river valley environments using airborne LiDAR data. *Earth Surface Processes and Landforms*, 32, 1574–1592.
- Kind, J. M. (2014). Economically efficient flood protection standards for the Netherlands. *Journal of Flood Risk Management*, 7(2), 103–117.
- Kondolf, M., Piégay, H., Schmitt, L., & Montgomery, D. (2016). Geomorphic classification of rivers and streams. In Kondolf, M., Piégay, H. *Tools in Fluvial Geomorphology*, 7, 133–158.
- Langhammer, J., & Vacková, T. (2018). Detection and mapping of the geomorphic effects of flooding using UAV photogrammetry. *Pure and Applied Geophysics*. doi:10.1007/s00024-018-1874-1.
- MacEachren, A. M. (2004). *How maps work. Representation, Visualization, and design* (p. 513). New York, NY: The Guilford Press.
- Miklín, J., & Galia, T. (2017). Detailed fluvial-geomorphologic mapping of wadeable streams: A proposal of universal map symbology. *Journal of Maps*, 13(2), 698–706.
- Montané, A. (2014). L'approche hydrogéomorphologique: pratiques, valorisations et développement d'une méthode de cartographie des zones inondables. PhD Thesis, Université Paul Valéry - Montpellier III.
- Ocio, D., Stocker, C., Eraso, A., Martínez, A., & Sanz de Galdeano, J. M. (2016). Towards a reliable and cost-efficient flood risk management: The case of the Basque Country (Spain). *Natural Hazards*, 81(1), 617–639.
- Ollero, A. (1991). Estudio ecogeográfico de los meandros del Ebro en el sector Rincón de Soto-Novillas. Ministerio de Obras Públicas y Transportes, 334 p., Madrid.
- Ollero, A. (1992). Los meandros libres del río Ebro (Logroño-La Zaida): geomorfología fluvial, ecogeografía y riesgos. PhD Thesis, Universidad de Zaragoza.
- Ollero, A. (2010). Channel changes and floodplain management in the meandering middle Ebro River, Spain. *Geomorphology*, 117, 247–260.
- Pellicer, F., & Ollero, A. (1987). Dinámica de los meandros del Ebro en la Rioja Baja (sector Alfaro-Arguedas). *Actas X Congreso Nacional de Geografía*, I: 57–66, Asociación de Geógrafos Españoles, Zaragoza.
- Piégay, H. (2016). System approaches in fluvial geomorphology. In Kondolf, M., Piégay, H. *Tools in Fluvial Geomorphology*, 5, 75–102.
- Rusnák, M., Sládek, J., Kidová, A., & Lehotský, M. (2018). Template for high-resolution river landscape mapping using UAV technology. *Measurement*, 115, 139–151.
- SNCZI. (2011). Guía Metodológica para el desarrollo del Sistema Nacional de Cartografía de Zonas Inundables. Ministerio de Medio Ambiente y Medio Rural y Marino, Madrid, 349 p.
- Tockner, K., & Stanford, J. A. (2002). Riverine flood plains: Present state and future trends. *Environmental Conservation*, 29, 308–330.
- Vinet, F. (2010). Le risque inondation. Diagnostic et gestion. Tec & Doc Lavoisier, 318 p., Paris.
- Wang, Z. (1996). Manual versus Automated Line Generalization. GIS/LIS '96 Proceedings, p. 94–106.
- Wheaton, J. M., Fryirs, K. A., Brierley, G., Bangen, S. G., Bouwes, N., & O'Brien, G. (2015). Geomorphic mapping and taxonomy of fluvial landforms. *Geomorphology*, 248, 273–295.